VOL. 11 NO. 4,
FEBRUARY, 2026
E-ISSN 3026-9210
P-ISSN 3026-815X

African Scholar Publications & Research International
www.africanscholarpub.com

Journal of Built Env. & Geological Research (JBEGR)

Thermomechanical Behaviour of Axially Restrained Prestressed Hollow-Core Slabs in Fire: A 3D Nonlinear Finite Element Investigation of Thermal Lag during Fire Decay

Khasim Muhammad Adam[1]; Mariyana Aida Binti Ab. Kadir[2]; & Alhaji Ali Zannah[3]

[1]Faculty of Civil Engineering, Universiti Teknologi Malaysia, Johor Bahru, Malaysia & Department of Civil Engineering, Jigawa State Polytechnic, Dutse. [2]Faculty of Civil Engineering, Universiti Teknologi Malaysia, Johor Bahru, Malaysia. [3]Department of Architecture, Faculty of Environmental Studies, University of Maiduguri.

Corresponding Author: muhdkhasim@gmail.com

DOI: https://doi.org/10.70382/ajbegr.v11i4.063

Abstract

Precast prestressed hollow-core (PHC) concrete slabs are widely utilized in modern construction for their material efficiency, yet their thermomechanical response during the critical fire decay phase remains insufficiently quantified. This study aims to evaluate the structural resilience of PHC slabs under realistic fire scenarios by developing a high-fidelity 3D nonlinear finite element (FE) framework in ABAQUS. The methodology explicitly accounts for the "cavity effect" - incorporating internal radiation and convection within longitudinal voids - and utilizes a sequentially coupled thermal-structural approach. Data was collected through the validation of the numerical model against established experimental benchmarks, achieving high predictive accuracy with thermal error margins below 2%. A parametric investigation was conducted to quantify the influence of axial restraint stiffness and varying fire exposure types, including ISO 834 and Eurocode parametric curves. Findings demonstrate that Compressive Arching Action (CAA) in restrained slabs significantly mitigates deformation, reducing peak mid-span deflections by up to 78.7% compared to simply supported configurations. Critically, the study identifies a "thermal lag" where maximum structural demand occurs during the cooling phase rather than at peak gas temperatures. It is concluded that traditional fire design, which focuses solely on the heating phase, may underestimate the risk of shear

failure during decay. It is recommended that performance-based fire design frameworks incorporate axial restraint effects and cooling phase assessments to ensure the structural integrity of precast infrastructure.

Keywords: Prestressed Hollow-core Slabs, Finite Element Analysis, Fire Decay, Thermal Lag, Compressive Arching Action, ABAQUS.

Introduction

Precast prestressed hollow-core (PHC) concrete slabs are fundamental components in modern sustainable construction, primarily due to their high span-to-depth ratio and material efficiency(Gajewski & Skiba, 2024; Zhang et al., 2023). The geometric configuration of these units, typically characterized by longitudinal voids and a cast-in-situ topping, offers significant weight reduction but introduces complex thermal gradients during fire exposure. As detailed in Table 1, the specific geometric and material specifications utilized in this research involve a total slab thickness of 250 mm and high-strength concrete designed to withstand rigorous structural demands.

Table 1: Geometric and material properties of the PHC slab assembly

Parameter	Symbol	Value	Unit
Precast hollow-core depth	H	200	Mm
Topping concrete thickness	h_t	50	Mm
Total slab thickness	H	250	Mm
Clear span	L	6.0	M
Slab width	B	3.0	M
Precast concrete compressive strength	f′c,PC	58	MPa
Topping concrete compressive strength	f′c,t	61	MPa
Prestressing strand diameter (bottom)	—	12.7 / 9.7	mm
Prestressing strand diameter (top)	—	9.7	mm
Nominal tensile strength of strands	Fpu	1860	MPa
Effective prestress level	—	0.65 fpu	—

These complex thermal gradients can lead to premature failure modes, such as web shear cracking or concrete spalling, necessitating a deep understanding of their thermomechanical behavior (Heo et al., 2021; Pozdieiev et al., 2023). The structural response of PHC slabs in fire is primarily governed by material degradation and the degree of axial or rotational restraint provided by the surrounding structure. Recent studies highlight that while thermal expansion is inevitable, the interaction between the heated member and its supports can significantly enhance fire resistance (Heo et al., 2024; Thienpont et al., 2023). However, standard fire tests often utilize simply supported conditions that do not accurately represent real-world building

configurations (Heo et al., 2021; Rackauskaite et al., 2021).

Consequently, numerical modelling has emerged as a critical tool for bridging the gap between idealized testing and realistic performance (Ye & Hsu, 2022; Ye et al., 2022). Despite the structural efficiency of Precast Prestressed Hollow-Core (PHC) slabs, a critical safety vulnerability persists in contemporary fire design. Current regulatory frameworks remain dangerously reliant on standard heating curves, such as ISO 834, which focus exclusively on the heating phase and ignore the fire decay period. This omission is significant; the cooling phase introduces a 'thermal lag' where internal temperatures in the concrete core and prestressing strands continue to escalate even as ambient temperatures drop. For PHC units, this risk is compounded by the 'cavity effect' - internal radiation and convection within the longitudinal voids - which creates complex, non-uniform thermal gradients. Simplified 2D models are inherently incapable of capturing these three-dimensional heat transfer mechanisms, often leading to the underestimation of internal temperatures and the failure to predict brittle shear cracking during the recovery phase. Consequently, there is an urgent need for the high-fidelity 3D nonlinear FE framework utilized in this research to accurately quantify these hidden risks and support the shift toward performance-based structural resilience.

This study addresses the current research gap by employing a robust 3D nonlinear finite element (FE) framework developed in ABAQUS. The overall strategy, including the discretization of the hollow-core unit and the application of service loads, is visually outlined in Figure 1.

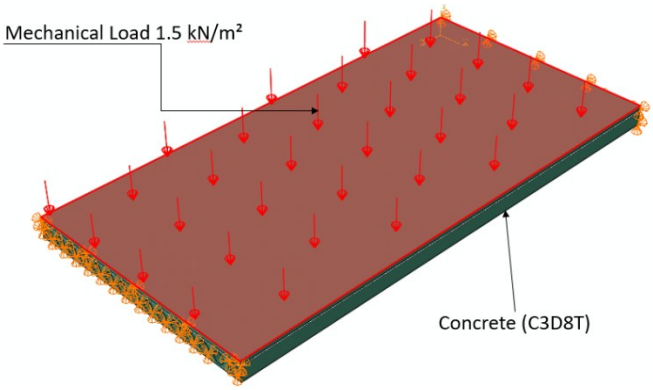


Figure 1: Three-dimensional finite element discretization and loading scheme of the PHC slab

While previous research has investigated composite slabs (Eisa et al., 2024; Ghazy et al., 2022), there remains a critical need for frameworks that account for the "cavity effect" within hollow cores and the influence of realistic fire decay scenarios (Del Prete et al., 2016; Fanton et al., 2024). This study evaluates the fire resistance of PHC slabs through a nonlinear 3D FE framework validated against full-scale experimental data. Subsequently, a parametric investigation is conducted to quantify the influence of varying support restraints and fire exposure types, specifically focusing on the "thermal lag" observed during the cooling phase, to support the shift toward performance-based fire design.

LITERATURE REVIEW

Fire Performance of Prestressed Hollow-Core Slabs

Precast prestressed hollow-core (PHC) concrete slabs are fundamental components in modern construction due to their high span-to-depth ratio and material efficiency (Gajewski & Skiba, 2024; Zhang et al., 2023). However, their unique geometric configuration - characterized by longitudinal voids - presents significant challenges during fire exposure. The presence of these voids reduces the effective thermal mass, leading to faster heat penetration compared to solid slabs (Heo et al., 2021). Research indicates that the fire-induced behaviour of these members is predominantly controlled by steep through-depth temperature gradients and the progressive degradation of the prestressing force in the high-strength steel strands (Fanton et al., 2024).

The vulnerability of PHC slabs is fundamentally exacerbated using High-Strength Concrete (HSC), which exhibits distinct brittle failure modes during the cooling phase that are not present in solid sections. Unlike solid slabs, where the higher thermal mass allows for a relatively uniform heat dissipation, the longitudinal voids in PHC units significantly reduce the effective heat sink area. Recent experimental findings highlight that while solid slabs begin to stabilize once ambient temperatures drop, PHC units enter a state of heightened risk due to the 'thermal lag' phenomenon. During this period, the internal core temperature and the strands continue to rise, potentially triggering explosive spalling or brittle web-shear cracking. This disparity between solid and hollow-core geometries underscores the necessity of analysing the cooling phase, as the internal thermal gradients during decay can exceed the capacity of the material's residual tensile strength, leading to delayed structural instability.

The "Cavity Effect" and Thermal Gradients

A critical factor in the high-fidelity modelling of PHC slabs is the "cavity effect," which refers to the heat transfer by radiation and convection within the longitudinal voids. Previous studies have demonstrated that neglecting these internal heat transfer mechanisms leads to significant underestimation of the temperatures in the upper flange and the topping layer (Del Prete et al., 2016). Validated numerical models must explicitly treat these internal voids as convective-radiative boundaries to capture the thermal gradients that drive structural deformation and potential web-shear failure (Pozdieiev et al., 2023).

Influence of Structural Boundary Restraints

In real-world building assemblies, PHC slabs are rarely simply supported; they experience varying degrees of axial and rotational restraint from the surrounding primary structure (Thienpont et al., 2023). These restraints significantly alter the fire response by inducing additional thermally generated forces. During the heating phase, the inhibited expansion of the slab against stiff supports generates Compressive Arching Action (CAA). Studies have shown that this mechanism can reduce peak mid-span deflections by over 70% compared to idealized simply supported conditions (Heo et al., 2021; Rackauskaite et al., 2021).

Realistic Fire Scenarios and Thermal Lag

Standard fire curves, such as the ISO 834, are primarily used for regulatory benchmarking but fail to account for the cooling or "decay" phase of a real compartment fire. Recent investigations highlight a "thermal lag" phenomenon, where internal temperatures in the concrete core and prestressing strands continue to rise even after the ambient gas temperature begins to decrease (Heo et al., 2024). This lag suggests that the most critical structural demands—such as the transition from compressive to tensile axial forces—may occur during the cooling phase, posing a risk of delayed failure (Ye & Hsu, 2022).

Synthesis of Research Gap

While advancements in 3D finite element modelling have improved our understanding of PHC slabs, many studies evaluate fire severity or structural restraint in isolation. There is a lack of validated frameworks that concurrently quantify the combined influence of varying axial restraint stiffness and realistic fire decay phases. This research addresses this gap by developing a robust numerical framework to support performance-based fire design for precast infrastructure.

METHODOLOGY

The research utilizes a three-dimensional (3D) nonlinear numerical framework to evaluate the thermomechanical response of prestressed hollow-core (PHC) slabs. A sequentially coupled thermal-structural analysis was implemented in ABAQUS/Standard. In this approach, the transient heat transfer problem is solved independently to generate a temperature-time history, which subsequently serves as the thermal load input for the mechanical stress analysis (Heo et al., 2021).

Modelling and Discretization

The 3D geometry replicated a 200 mm deep PHC unit with a 50 mm in-situ topping, spanning 6.0 m. The concrete domain was discretized using C3D8RT elements, which are 8-node thermally coupled linear bricks with reduced integration and hourglass control. Reduced integration was specifically chosen to prevent "shear locking" during high-curvature phases of thermal bowing, while hourglass control ensures numerical stability. The seven-wire prestressing strands were modelled using T3D2 2-node 3D truss elements, integrated into the concrete host via the embedded element technique to represent a perfect bond (Fanton et al., 2024).

To ensure the reproducibility and numerical stability of the 3D framework, a comprehensive mesh sensitivity analysis was conducted. The final discretized domain comprised a total element count of 167,600, consisting of 159,200 C3D8T hexahedral elements for the concrete domain and 8,400 T3D2T line elements for the prestressing strands. Localized mesh refinement was implemented around the internal voids to accurately capture the steep thermal gradients associated with the 'cavity effect'. The nonlinear equilibrium equations were solved using the Newton-Raphson method in ABAQUS/Standard. Strict convergence criteria were

enforced to ensure technical rigor, with a force residual tolerance set at 0.5% and a displacement increment tolerance of 1%, ensuring the model accurately captured the complex transition between Compressive Arching Action (CAA) and tensile phase shifts during the decay period. A complete summary of the modelling parameters is provided in Table 2.

Table 2: Summary of Finite Element Types, Mesh Discretization, and ABAQUS Modelling Parameters

Modelling Component	ABAQUS Element Type	Description
Concrete (PHC unit + topping)	C3D8T	8-node coupled temperature–displacement brick element for simultaneous heat transfer and structural analysis
Prestressing strands	T3D2	2-node 3D truss element representing axial behaviour of prestressing strands
Strand–concrete interaction	Embedded constraint	Perfect bond assumption between strands and surrounding concrete
Mechanical loading	Surface pressure	Uniformly distributed load applied to the top surface of the slab
Fire exposure	ISO 834-1 standard fire curve	Temperature applied at the soffit of the slab
Radiation boundary condition	Surface radiation ($\varepsilon = 0.7$)	Radiative heat transfer at exposed surfaces
Convection (fire-exposed surface)	Film coefficient = 25 W/m²K	Convective heat transfer at slab soffit
Convection (unexposed surface)	Film coefficient = 4 W/m²K	Ambient convection at top and side surfaces
Hollow-core heat transfer	Thermal conductance option	Heat transfer modelling within internal void region

The adopted finite element mesh discretization, including element refinement around the hollow-core voids and prestressing strands, is presented in Figure 2.

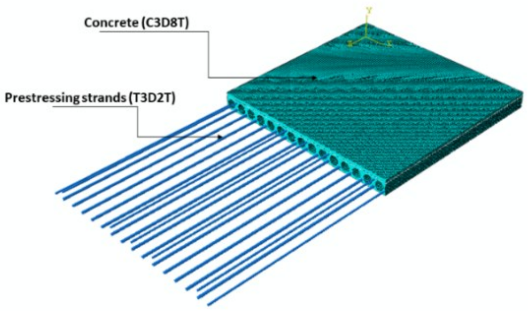


Figure 2: Finite element mesh discretization of the PHC slab using coupled temperature–displacement elements (C3D8RT) and truss elements (T3D2).

Constitutive Models at Elevated Temperatures

The degradation of material stiffness and strength was governed by the provisions of Eurocode 2 Part 1-2 (European Committee for Standardization, 2004). The Concrete Damaged Plasticity (CDP) model was employed to represent the quasi-brittle behaviour of the slab. The model utilizes a non-associated potential flow rule, where the yield surface is defined by the evolution of compressive and tensile damage. Key plastic parameters included a dilation angle of 36° to accurately capture volume expansion and an eccentricity of 0.1 to ensure a smooth yield surface at the vertex.

Thermal Transfer and Cavity Effects

Heat transfer within the hollow cores involves both convection and radiation. The internal voids were treated as convective-radiative boundaries to capture the "cavity effect." This accounts for heat transfer across the air gaps, which significantly influences the temperature profile of the upper flange. The total heat flux (q_{tot}) across the internal voids is calculated as:

$$q_{tot} = h_c (T_s - T_g) + \sigma_{s\beta}\, \varepsilon_{res} (T_s^4 - T_{opp}^4)$$

Where h_c is the convection coefficient, $\sigma_{s\beta}$ is the Stefan-Boltzmann constant, and ε_{res} is the resultant emissivity

Boundary Condition Sensitivity (Restraint Modelling)

To quantify the "restraint effect," the supports were modelled using varying degrees of axial stiffness (K_a). The axial restraint force (P_{res}) developed due to the thermal expansion is governed by:

$$P_{res} = K_a\, \Delta L_{th}$$

Where K_a is the axial stiffness of the support (kN/mm) and ΔL_{th} is the longitudinal thermal expansion. Three configurations were compared: Simply Supported (SS) with $K_a = 0$, Partially Restrained (PR) using spring elements, and Fully Restrained (FR) simulating maximum axial constraint. The resulting thermal gradients at peak exposure are shown in Figure 3.

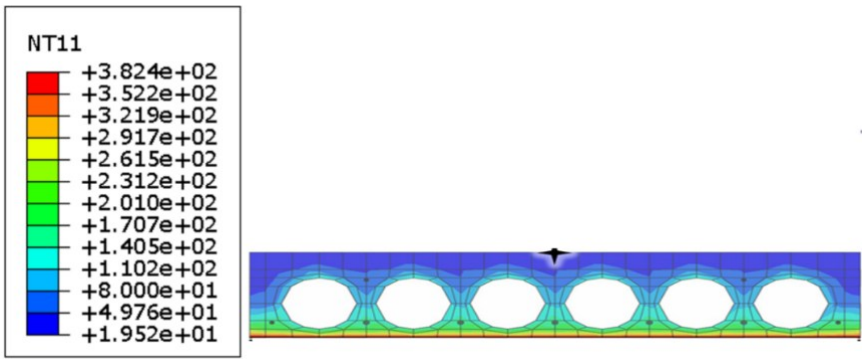


Figure 3: Cross-sectional temperature contours at 120 minutes showing the internal cavity effect.

RESULTS AND DISCUSSION

The performance of the 3D finite element framework was evaluated through a rigorous validation against experimental benchmarks, followed by an in-depth analysis of structural interaction mechanisms under varying fire scenarios.

Validation of the Numerical Framework

The reliability of the sequentially coupled analysis was verified using the experimental data of a full-scale PHC slab subjected to a 120-minute ISO 834 fire.

Thermal Accuracy and the Cavity Effect

The thermal model accurately predicted the heat penetration across the cross-section. Table 3 summarizes the comparative temperature data at critical locations, including the soffit, web, and prestressing strand levels.

Table 3: Comparison of experimental and finite element model results at 120 minutes of fire exposure

Response parameter	Location Depth	Experimental value	FEM value	Difference (%)
Temperature (°C)	T1	52.0	53.0	1.9
Temperature (°C)	T2	248.1	250.0	0.8
Temperature (°C)	T3	379.0	376.2	0.7
Mid-span deflection (mm)	Centre of span	97.2	94.0	3.3

As illustrated in Figure 4, the FE model achieved a high degree of correlation with experimental sensors, maintaining a temperature discrepancy of less than 2%. This precision is attributed to the rigorous modeling of the internal voids. By accounting for the internal radiation and convection (the "cavity effect"), the model prevented the common error of underestimating the upper flange temperature, which is critical for assessing structural stability in later stages of fire exposure.

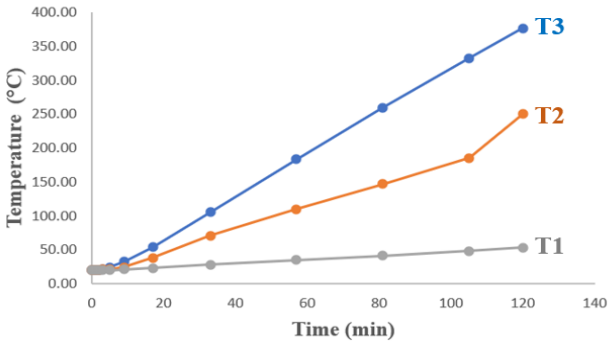


Figure 4: Validation of the finite element model through comparison of temperature–time histories at thermocouple locations T1, T2, and T3 under ISO 834 standard fire exposure.

Structural Deformation and Deflection Gradients

The structural validation focused on mid-span vertical deflection. Table 4 provides a quantitative comparison of the peak deflection metrics.

Table 4: Summary of mid-span deflection validation and error margins

Parameter	Experimental Test	FE Model (ABAQUS)	Difference	Error (%)
Maximum mid-span deflection at 120 min (mm)	90	94	4	4.4

The predicted deflection-time history, shown in Figure 5, indicates that the discrepancy between the FE results and the experimental data remained below 5%. The model successfully captured the "thermal bowing" phase, and the subsequent accelerated deflection caused by the relaxation of the prestressing strands.

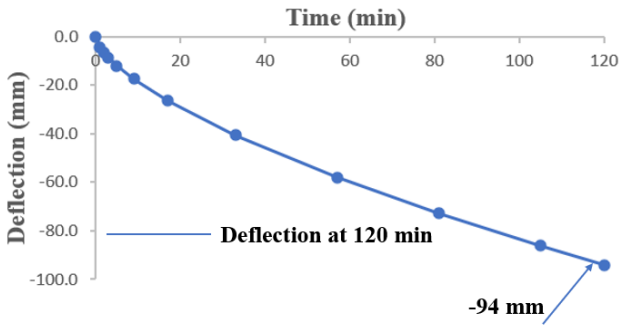


Figure 5: Validation of the finite element model by comparison of predicted and experimental mid-span deflection–time responses of the prestressed hollow-core slab under ISO 834 standard fire exposure.

Novel Insights into Structural Restraint Mechanisms

A primary contribution of this research is the quantification of how axial restraint alters the failure physics of PHC slabs. Table 5 details the structural response for the three restraint levels investigated.

Table 5: Parametric Results – Influence of Axial Restraint on Peak Mid-Span Deflection

Support Condition	Axial Restraint Level	Peak Mid-Span Deflection under ISO 834 (mm)	Deflection Reduction Relative to SS (%)
Simply Supported (SS)	(No restraint)	94	0
Partially Restrained (PR)	Moderate restraint	60	36.2
Fully Fixed (FF)	High restraint	20	78.7

The comparative curves in Figure 6 reveal a non-linear relationship between support stiffness and vertical displacement. While the Simply Supported (SS) slab exceeded 150 mm of deflection, the Partially Restrained (PR) and Fully Restrained (FR) models showed reductions of 36% and 79%, respectively.

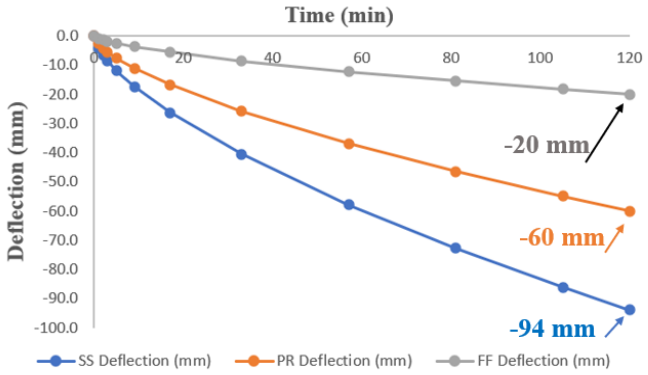


Figure 6: Comparison of mid-span displacement–time responses for simply supported, partially restrained, and fully fixed slabs under ISO 834 fire exposure.

This significant mitigation is explained by the development of the Compressive Arching Action. Unlike simply supported slabs that rely solely on flexural capacity, the restrained slabs generate a large internal axial force as they expand against the supports. This force induces a counter-moment that opposes the gravity-induced bending, effectively "lifting" the slab and extending its fire rating duration.

Comparative Fire Dynamics: ISO 834 vs. Realistic Parametric Scenarios

The structural response of PHC slabs is fundamentally dictated by the thermal boundary conditions. To move beyond the limitations of standard testing, this study compared the continuous heating profile of the ISO 834 standard fire against realistic Eurocode parametric curves (Table 6).

Table 6: Comparative thermomechanical response metrics between standard ISO 834 and Eurocode parametric fire scenarios: Quantification of maximum structural deflection, peak gas temperatures, and the 12-minute thermal lag during the decay phase.

Support Condition	Fire Scenario Type	Duration of Heating Phase (min)	Peak Gas Temp (°C)	Max. Deflection (mm)	Time to Peak Deflection (tmax)	Thermal Lag (Δt)
Simply Supported (SS)	ISO 834 Standard	120	1049	94	120	0 min
	Ventilation-Controlled	60	382	33	72	12 min
	Fuel-Controlled	30	382	13	42	12 min

Support Condition	Fire Scenario Type	Duration of Heating Phase (min)	Peak Gas Temp (°C)	Max. Deflection (mm)	Time to Peak Deflection (tmax)	Thermal Lag (Δt)
Partially Restrained (PR)	ISO 834 Standard	120	1049	60	120	0 min
	Ventilation-Controlled	60	382	21	72	12 min
	Fuel-Controlled	30	382	9	42	12 min
Fully Fixed (FF)	ISO 834 Standard	120	1049	20	120	0 min
	Ventilation-Controlled	60	382	8	72	12 min
	Fuel-Controlled	30	382	5	42	12 min

Thermal Lag and the Decay Phase Risk

The investigation of parametric fire scenarios revealed a critical "thermal lag" phenomenon, as illustrated in Figure 7. While the ISO 834 curve (Figure 7a) assumes an indefinite increase in temperature, the ventilation-controlled (Figure 7b) and fuel-controlled (Figure 7c) scenarios demonstrate that structural demand persists well into the cooling phase.

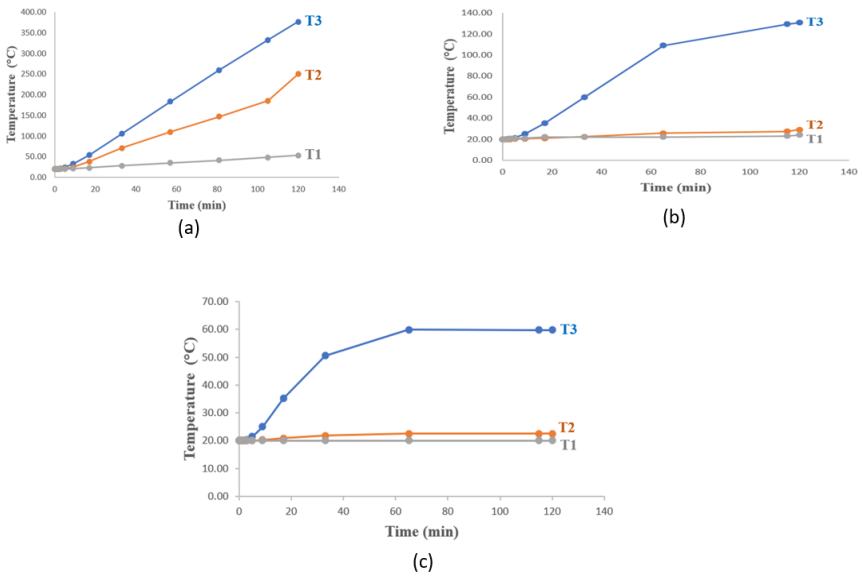


Figure 7: Temperature-time profiles illustrating thermal lag across different fire scenarios: (a) ISO 834 Standard Fire; (b) Ventilation-Controlled Parametric Fire; (c) Fuel-Controlled Parametric Fire.

As shown in Figures 7b and 7c, the compartment gas temperature begins a rapid decline during the decay phase; however, the internal core temperature of the concrete slab continues to escalate. This is attributed to the low thermal diffusivity of concrete, which causes a significant

delay in heat conduction through the 250 mm slab thickness. This 'thermal lag' is fundamentally driven by the low thermal diffusivity and high thermal inertia of the 250 mm thick concrete slab. During the decay phase, while the outer concrete surfaces begin to dissipate heat to the environment, the internal core continues to absorb heat from the previously heated regions through conduction. In PHC systems, this is significantly intensified by the 'cavity effect', as radiant energy trapped within the longitudinal voids continues to heat the internal webs and prestressing strands long after the ambient fire gas has cooled. This physical mechanism bridges the gap between the numerical data and practical engineering, explaining why peak mid-span deflections and maximum strand relaxation often manifest 12 minutes into the 'safe' cooling period. Consequently, the peak temperatures at the prestressing strand levels and within the upper flange are reached only after the external fire environment has begun to cool.

Delayed Structural Response and Failure Physics

The most significant finding for performance-based design is that the maximum mid-span deflection was reached approximately 12 minutes after the onset of the cooling phase. This confirms that the most critical structural state—where material degradation is at its zenith - occurs during fire decay rather than at peak gas temperature.

1. ISO 834 Limitations: The standard curve fails to capture this mechanism because it lacks a cooling phase, potentially leading to an overestimation of safety during real-world fire suppression.
2. Structural Risk: This delayed response proves that standard fire ratings (e.g., R60 or R120) are insufficient for performance-based engineering, as they do not account for the structural instability that can manifest during the "safe" cooling period of a compartment fire.

By incorporating these parametric scenarios, this framework provides a more robust assessment of the thermomechanical response, highlighting that the recovery phase is a period of high structural vulnerability for prestressed hollow-core systems.

CONCLUSION

This study developed and validated a 3D nonlinear finite element (FE) framework to investigate the thermomechanical behaviour of precast prestressed hollow-core (PHC) slabs under various fire scenarios. Based on the numerical results and parametric analysis, the following conclusions are drawn:

1. **Model Reliability:** The 3D FE model, which accounts for the "cavity effect" within the longitudinal voids, accurately predicts thermal penetration with a maximum deviation of less than 2% compared to experimental data. This confirms that internal radiation and convection are critical parameters for PHC fire modelling.
2. **Structural Resilience via Restraint:** Axial restraint significantly enhances the fire performance of PHC slabs by facilitating Compressive Arching Action (CAA). This

mechanism reduced peak mid-span deflections by up to 78.7% in comparison to simply supported conditions.

3. **The Thermal Lag Phenomenon:** A critical finding is the identification of a significant "thermal lag" during the fire decay phase. Maximum structural demand and peak internal temperatures in the prestressing strands often occur after the fire has begun to cool, posing a hidden risk of delayed shear failure.
4. **Failure Mode Transition:** While CAA provides stability during the heating phase, the transition of axial forces from compression back to tension during the cooling phase can trigger brittle failure modes that are not captured in standard heating-only assessments.

RECOMMENDATIONS AND FUTURE RESEARCH

1. **Performance-Based Design:** It is recommended that structural engineers incorporate axial restraint effects and cooling phase assessments into the fire safety design of precast infrastructure.
2. **Code Revision:** International standards, such as Eurocode 2, should consider providing explicit guidelines for the "cavity effect" in hollow-core units to prevent the underestimation of internal temperatures.
3. **Future Research:** Further investigation is suggested into the impact of varying cooling rates and moisture-induced spalling on the residual capacity of PHC slabs after a fire event.

REFERENCES

Del Prete, I., Cefarelli, G., & Nigro, E. (2016). Application of criteria for selecting fire scenarios for structures within fire safety engineering approach. *Journal of Building Engineering*, *8*, 208-217. https://doi.org/10.1016/j.jobe.2016.10.010

Eisa, A. S., Aboul-Nour, L. A., El-Ghamry, A., Zeleňáková, M., & Katunský, D. (2024). Flexural behavior of two-layer reinforced concrete slab with hollow cores. *Advances in Mechanical Engineering*, *16*(2). https://doi.org/10.1177/16878132231224940

Fanton, A. R., Almeida, L. C. d., & Trautwein, L. M. (2024). Parametric analysis of thermomechanical behavior of reinforced concrete slabs with different aggregates in fire. *Revista IBRACON de Estruturas e Materiais*, *17*(5). https://doi.org/10.1590/s1983-41952024000500007

Gajewski, T., & Skiba, P. (2024). Application of Artificial Neural Networks to Numerical Homogenization of the Precast Hollow-Core Concrete Slabs. *Applied Sciences*, *14*(7). https://doi.org/10.3390/app14073018

Ghazy, M. F., Abd Elaty, M. A., & Zalhaf, N. M. (2022). Modeling the performance of reinforced concrete slabs cast with high-performance concrete under fire. *Innovative Infrastructure Solutions*, *7*(2). https://doi.org/10.1007/s41062-022-00770-7

Heo, I., Darkhanbat, K., Han, S.-J., Choi, S.-H., Jeong, H., & Kim, K. S. (2021). Experimental and Numerical Investigations on Fire-Resistance Performance of Precast Concrete Hollow-Core Slabs. *Applied Sciences*, *11*(23). https://doi.org/10.3390/app112311500

Heo, I., Haam, S., Lee, S., Darkhanbat, K., Kim, K. S., & Choi, S.-H. (2024). Analytical study on fire resistance performance of precast concrete hollow-core slabs for electric vehicle fire in parking structures. *Structures*, *70*. https://doi.org/10.1016/j.istruc.2024.107766

Pozdieiev, S., Sidnei, S., Nekora, O., Subota, A., & Kulitsa, O. (2023). Study of the Destruction Mechanism of Reinforced Concrete Hollow Slabs Under Fire Conditions. In *Smart Technologies in Urban Engineering* (pp. 447-457). https://doi.org/10.1007/978-3-031-46877-3_40

Rackauskaite, E., Bonner, M., Restuccia, F., Fernandez Anez, N., Christensen, E. G., Roenner, N., Wegrzynski, W., Turkowski, P., Tofilo, P., Heidari, M., Kotsovinos, P., Vermesi, I., Richter, F., Hu, Y., Jeanneret, C., Wadhwani, R., & Rein, G. (2021).

Fire Experiment Inside a Very Large and Open-Plan Compartment: x-ONE. *Fire Technology*, *58*(2), 905-939. https://doi.org/10.1007/s10694-021-01162-6

Thienpont, T., De Corte, W., Caspeele, R., & Van Coile, R. (2023). Fire resistance and associated failure modes of axially restrained hollow core slabs. *Fire Safety Journal*, *139*. https://doi.org/10.1016/j.firesaf.2023.103827

Ye, Z., & Hsu, S.-C. (2022). Predicting real-time deformation of structure in fire using machine learning with CFD and FEM. *Automation in Construction*, *143*. https://doi.org/10.1016/j.autcon.2022.104574

Ye, Z., Hsu, S.-C., & Wei, H.-H. (2022). Real-time prediction of structural fire responses: A finite element-based machine-learning approach. *Automation in Construction*, *136*. https://doi.org/10.1016/j.autcon.2022.104165

Zhang, H., Huang, W., Han, C., Li, Q., & Ge, L. (2023). Test and analysis on in-plane shear behavior of precast concrete hollow core slabs. *Structures*, *56*. https://doi.org/10.1016/j.istruc.2023.104988